

1 **Effects of fertilization and stand age on N₂O and NO emissions from** 2 **tea plantations: A site-scale study in a subtropical region using a** 3 **modified biogeochemical model**

4 Wei Zhang¹, Zhisheng Yao¹, Xunhua Zheng^{1, 2}, Chunyan Liu¹, Rui Wang¹, Kai Wang¹, Siqi Li¹,
5 Shenghui Han¹, Qiang Zuo³, Jianchu Shi³

6 ¹ State Key Laboratory of Atmospheric Boundary Layer Physics and Atmospheric Chemistry, Institute of Atmospheric
7 Physics, Chinese Academy of Sciences, Beijing 100029, P. R. China

8 ² University of Chinese Academy of Sciences, Beijing 100049, P.R. China

9 ³ College of Resources and Environmental Sciences, China Agricultural University, Beijing 100193, P.R. China

10 *Corresponding to:* Xunhua Zheng (xunhua.zheng@post.iap.ac.cn); Zhisheng Yao (zhishengyao@mail.iap.ac.cn)

11 **Abstract.** To meet increasing demands, tea plantations are rapidly expanding in China. Although the emissions of nitrous
12 oxide (N₂O) and nitric oxide (NO) from tea plantations may be substantially influenced by soil pH reduction and intensive
13 nitrogen fertilization, process model-based studies on this issue are still rare. In this study, the process-oriented
14 biogeochemical model, Catchment Nutrient Management Model - DeNitrification-DeComposition (CNMM-DNDC), was
15 modified by adding tea growth-related processes that may induce a soil pH reduction. Using a dataset for intensively
16 managed tea plantations at a subtropical site, the performances of the original and modified models for simulating the
17 emissions of both gases subject to different fertilization alternatives and stand ages were evaluated. Compared with the
18 observations in early stage of a tea plantation, the original and modified models showed comparable performances for
19 simulating the daily gas fluxes (with Nash-Sutcliffe index (NSI) of 0.10 versus 0.18 for N₂O and 0.32 versus 0.33 for NO),
20 annual emissions (with NSI of 0.81 versus 0.94 for N₂O and 0.92 versus 0.94 for NO) and annual direct emission factors
21 (EF_ds). For the modified model, the observations and simulations demonstrated that short-term replacement of urea with
22 oilcake stimulated N₂O emissions by ~62% and ~36% and mitigated NO emissions by ~25% and ~14%, respectively. The
23 model simulations resulted in a positive dependence of EF_d of either gas against nitrogen doses, implicating the importance
24 of model-based quantification of this key parameter for inventory. In addition, the modified model with pH-related scientific
25 processes showed overall inhibitory effects on the gases emissions in the mid to late stages during a full tea lifetime. In
26 conclusion, the modified CNMM-DNDC exhibits the potential for quantifying N₂O and NO emissions from tea plantations
27 under various conditions. Nevertheless, wider validation is still required for simulation of long-term soil pH variations and
28 emissions of both gases from tea plantations.

29 1 Introduction

30 Tea (*Camellia sinensis* (L.) Kuntze), as a perennial cash crop, has been widely cultivated long-term in the tropical and
31 subtropical regions of the world, with nearly 90% of the global tea harvest area currently located in Asia and over 50% of
32 that located within China (<http://www.fao.org/faostat/>). To maximize the economic benefits, especially in China, tea
33 production has expanded intensively, mostly through the conversion of arable uplands, rice paddies and forests into tea
34 plantations (e.g., Xue et al., 2013; Yao et al., 2015). For instance, both the total harvest area and production have
35 dramatically increased by 166% (from 1.09×10^6 to 2.90×10^6 ha) and 253% (from 6.8×10^5 to 2.40×10^6 Mg), respectively,
36 from 2000 to 2016 (<http://www.fao.org/faostat/>).

37 As a leaf/bud-harvested crop, nitrogen is the key nutrient for yield. Thus, high tea yields are largely supported by the
38 intensive application of nitrogen fertilizers. The nitrogen inputs amount to 450–1200 (mean: 553) kg N ha⁻¹ yr⁻¹ in the
39 primary areas of tea cultivation in China (Han et al., 2013), which is much higher than the recommended doses of 250–375
40 kg N ha⁻¹ yr⁻¹ (Fu et al., 2012; Hirono and Nonaka, 2012, 2014; Hou et al., 2015; Li et al., 2016; Tokuda and Hayatsu, 2004;
41 Yamamoto et al., 2014; Yao et al., 2015, 2018). This intensive nitrogen application results in superfluous reactive nitrogen
42 remaining in the soil. The excessive reactive nitrogen induces the high potential for nitrous oxide (N₂O) and nitric oxide (NO)
43 emissions, thus leading to the detrimental consequences of global warming and air pollution.

44 The tea plant has been well known as one of the very few families tolerable to high levels of aluminum ion (Al³⁺) and
45 thus can grow well in acidic soil (Taylor, 1991). Mature leaves of the tea plant may contain up to 30 g Al kg⁻¹ on dry weight
46 basis (Matsumoto et al., 1976) without experiencing Al toxicity (Morita et al., 2008). Part of the tissue Al further returns to
47 soil through plant trimming and thus leads to Al accumulation in surface soil of a tea plantation. In addition, the Al under an
48 acidic condition can be recombined with the organic matter derived from root exudation. This process further facilitates the
49 accumulation of Al in the upper soil layer of a tea plantation (Lin et al., 2014). The former mechanism of Al accumulation
50 in surface soil almost does not occur for the absolutely majority of plant families that much more weakly absorption of Al
51 than tea plant (Taylor, 1991; Matsumoto et al., 1976). Hence, the soil pH of tea plantations decreases with the increased
52 stand age jointly due to the processes of (i) acid release by root exudation and (ii) hydrogen ion (H⁺) production in the
53 hydrolysis of the accumulated Al³⁺ from residue decomposition in surface soil. The high nitrogen doses combined with the
54 decreased soil pH may further promote the production of the harmful nitrogenous gases through both microbial processes
55 (e.g., nitrification and denitrification) and non-biological mechanisms (e.g., chemo-denitrification) (e.g., Chen et al., 2017;
56 Fu et al., 2012; Yao et al., 2018), especially for the low pH. A number of field studies have demonstrated that much more
57 N₂O and NO were emitted from tea plantations than those in other upland fields (e.g., Akiyama et al., 2006). In China, the
58 N₂O and NO emissions from tea plantations are 16.6 and 14.9 kg N ha⁻¹ yr⁻¹ on average, respectively (Fu, 2013; Han et al.,
59 2013; Yao et al., 2015, 2018). In 2013, for instance, the N₂O emissions from tea plantations in China accounted for more
60 than one-tenth of the national total emissions of this gas from croplands and contributed to 85% of the total N₂O emissions
61 from global tea plantations (Li et al., 2016). To alleviate the negative impacts on environmental quality and human health,

62 organic fertilization has been strongly recommended in China and adopted in nearly 4.5×10^4 ha of tea fields by 2011 (Han et
63 al., 2013). Application of organic fertilizers in tea fields can improve soil fertility (e.g., Han et al., 2013), while stimulating
64 N_2O emissions but mitigating NO release (Yao et al., 2015). Therefore, investigating the impacts of replacing synthetic
65 nitrogen fertilizer with organic manure and the effect of stand ages on the emissions of N_2O and NO from tea plantations is
66 necessary for understanding the mechanisms of nitrogen cycling and effectively mitigating the emissions of both of the
67 nitrogenous gases from tea fields.

68 Compared with time- and labor-consuming field experiments, from which first-hand information of N_2O and NO
69 emissions could be obtained, modeling approaches based on sufficient validation have been proposed to overcome the limits
70 of field measurements (e.g., Chen et al., 2017). Because process-oriented biogeochemical models such as DNDC (e.g., Li,
71 2000), LandscapeDNDC (e.g., Haas et al., 2012), WNMM (e.g., Li et al., 2007) and CNMM-DNDC (Zhang et al., 2018) are
72 generally designed following the basic theories of physics, chemistry, physiology and biology, they are expected to be
73 widely applicable under various climates, soils, land uses and field management practices. These models, in principle, can
74 facilitate the understanding of the interactions among various processes, identify gaps in current knowledge, and
75 temporally/spatially extrapolate the results from experiments (Chen et al., 2008). Among these models, the Catchment
76 Nutrient Management Model - DeNitrification-DeComposition (CNMM-DNDC) is one of the latest versions of the DNDC.
77 CNMM-DNDC was established by incorporating the core carbon and nitrogen biogeochemical processes of DNDC
78 (including the processes of decomposition, nitrification, denitrification and fermentation) into the hydrologic framework of
79 the CNMM, and it therefore inherited the features from both CNMM and DNDC (Zhang et al., 2018). CNMM-DNDC was
80 established to solve a common bottleneck problem of most biogeochemical models, i.e., the inability to simulate the lateral
81 flows of water and nutrients. This solution potentially enables the model to identify the best management practices of
82 intensive cropping systems. In its initial validation in a catchment with calcareous soils and complex landscapes, the
83 CNMM-DNDC performed fairly well in simulating ecosystem productivity (represented by crop yields in croplands),
84 hydrological nitrogen losses by soil leaching and nitrate discharge in streams, and emissions of gaseous carbon (carbon
85 dioxide, methane) and nitrogenous gases (N_2O , NO and ammonia) from different lands (forests and arable lands cultivated
86 with maize, wheat, oil rape, or paddy rice) (Zhang et al., 2018). However, the scientific processes of soil pH reduction due to
87 tea growth is still lacking in the CNMM-DNDC. This gap may induce significant biases in simulating the fluxes of both
88 nitrogenous gases from tea fields, especially for long term prediction, because soil pH is the key factor regulating N_2O and
89 NO emissions from the soil (e.g., Chen et al., 2017; Yao et al., 2018). Therefore, the authors hypothesize that adding the
90 missing scientific processes which lead to soil pH reduction into the internal model program codes can improve the
91 performance of the CNMM-DNDC in simulating the N_2O and NO emissions from tea plantations with different stand ages.
92 Filling the gap in the model is especially necessary for predicting the long term emissions of both gases from tea plantations.

93 To test the above hypothesis, the authors conducted a case study using a unique experimental dataset, which was
94 obtained by Yao et al. (2015, 2018) in a tea plantation with field treatments of fertilization alternatives and stand ages. The
95 aims of this case study were to (i) attempt to fill the gap in the CNMM-DNDC through addition of the processes that may

96 induce soil pH reduction due to tea growth, (ii) compare the performances of original and modified models in simulating
97 N_2O and NO emissions, and (iii) evaluate the modified model performance in simulating the direct emission factors (EF_d s) of
98 different annual nitrogen doses, and the N_2O and NO emissions affected by short-term replacement of a widely applied
99 synthetic nitrogen fertilizer (urea) with a typical organic manure (oilcake) and by the stand ages within the early stage (1–6
100 years) of a new tea plantation.

101 **2 Materials and methods**

102 **2.1 Introduction to the field site and experimental treatments**

103 The field site ($32^\circ 7.37' \text{N}$, $110^\circ 43.18' \text{E}$, 441 m above sea level) selected for this modeling case study is located in
104 Fangxian county, Hubei province, China. The field site is subject to a northern subtropical monsoon climate, with annual
105 precipitation of 914 mm and a mean air temperature of 14.2°C in 2003–2011 (Yao et al., 2015). Two plots at the field site
106 were involved in this study, encoded as T08 and T12, respectively. Both lands had been consecutively long-term cultivated
107 with paddy rice in summer and upland crops (or drained but fallowed) in winter until tea seedlings were transplanted in
108 March 2008 for T08 or March 2012 for T12. Conventional fertilization practices had been adopted in both plots. A typical
109 synthetic fertilizer (urea) was regularly applied at 450 (150 in autumn and 300 in spring) $\text{kg N ha}^{-1} \text{yr}^{-1}$ (encoded as T08-UN
110 and T12-UN). To determine the annual EF_d (the fraction of the applied fertilizer nitrogen released in the form of N_2O or NO
111 within the one-year period after fertilization) of either gas and to investigate the effects of short-term synthetic fertilizer
112 replacement by organic manure on N_2O and NO emissions, eight spatially replicated subplots were randomly set in either
113 T08 or T12: four for the control without nitrogen fertilizer applied (NN) and the others for exclusive application of organic
114 manure (OM) in 2013 (only T08) and 2014 (both T08 and T12). Each daily flux was inferred from the single measurement
115 based on five gas samples from a 30-min enclosure of a static opaque chamber between 09:00 and 11:00 (Beijing time).
116 Oilcake, one of the most widely applied organic manures in the subtropical regions of China, was exclusively amended in
117 the OM subplots to fully replace the urea, and nitrogen doses with the urea application outside the NN and OM subplots of
118 either plot. The NN and OM treatments were encoded as T08-NN, T08-OM, T12-NN, and T12-OM. T08-NN and T08-OM
119 were adopted consecutively in two full years (from October 2012 to March 2014), and T12-NN and T12-OM in one full year
120 (from October 2013 to March 2014). The organic manure in dry weight contained 7.1% nitrogen and 43.3% carbon. The
121 topsoil (0–15 cm depth) of the T08 and T12 plots had a loamy texture measured in 2013, and the detailed information was
122 provided in the online supplementary materials (Table S1). The soil pH at the time of tea seedling transplanting was 6.0 (Yao
123 et al., 2018). Irrigation was adopted following the typically regional management practice. Daily fluxes of N_2O and NO ,
124 topsoil (5 cm) temperature and surface soil (0–6 cm) moisture in water-filled pore space (WFPS) for each field treatment
125 were observed over two full years for T08-NN, T08-UN, and T08-OM (from mid-September 2012 to mid-October 2014) and
126 one full year for T12-NN, T12-UN, and T12-OM (from mid-September 2013 to mid-October 2014). For more detailed
127 information on the field experiments and observed data, refers to Yao et al. (2015, 2018) and Table S2.

128 **2.2 Model modifications**

129 In this study, the CNMM-DNDC was modified through (i) defining and applying a soil pH regulating factor (f_{sph}) on
 130 plant growth and (ii) adding two processes that produce H^+ and thus acidify soils (Miao, 2015; Pang, 2014). These
 131 modifications were made to enable the model to simulate the responses and feedbacks between tea growth and soil pH
 132 changes.

133 Considering that the soil pH for tea growth is optimal within 5.0–5.4 and suitable within 4.0–6.5 (Cao et al., 2009), f_{sph} ,
 134 a dimensionless factor (0–1), is newly parameterized as a quadratic polynomial function utilizing an average soil pH of 0–20
 135 cm (sph_a) as its single independent variable (Eq. 1). Based on Eq. 1, the value of f_{sph} is around 1.0 when soil pH is within
 136 5.0–5.4, and is above 0.85 when soil pH is within 4.0–6.5. However, the transient soil pH increase induced by urea
 137 hydrolysis is not considered for affecting plant growth, which can be offset due to the soil buffering effect within a few days.
 138 At each time step of simulation, the value of sph_a is updated. This parameterized factor is introduced into the model to
 139 regulate photosynthesis and thus plant growth, even though the modification to the model was not yet calibrated or validated
 140 due to a lack of sufficient field observations at the selected tea fields.

$$f_{\text{sph}} = -0.089\text{sph}_a^2 + 0.947\text{sph}_a - 1.51 \quad (1)$$

141 The two processes newly introduced into the model to simulate additional changes in the H^+ concentration ($\Delta[\text{H}^+]$),
 142 thus modifying soil pH, are (i) ionization of the amino acids and other organic acids (HR) in root exudates (Rxn 1) and (ii)
 143 hydrolysis of the Al^{3+} from the decomposition of tea residues due to the trimming (tea leaves and young branch) or falling of
 144 old leaves (Rxn 2).



145 The ionization equilibrium of organic acids is formulated in Rxn 1, wherein HR represents the category of amino acids
 146 or other organic acids in root exudates. Following Eqs. 2–4, the H^+ concentration changes due to the ionization of these
 147 exudate-contained acids ($\Delta[\text{H}^+]_{\text{ex}}$, mol L^{-1}) are calculated by solving the equations (analytical method) of Eqs. 3–4, which
 148 include the parameters of average ionization equilibrium constants for amino acids (K_{ami} , mol L^{-1}) and the other organic
 149 acids (K_{org} , mol L^{-1}) in root exudates and the molar concentrations of amino acids and organic acids in the soil water (c_{ami}
 150 and c_{org} , respectively, in mol L^{-1}). As the acid ionizations are thermodynamic processes, both K_{aim} and K_{org} vary with soil
 151 temperature (T , in $^{\circ}\text{C}$). Their values at various temperature conditions are given via the correction of their constant values at
 152 25 $^{\circ}\text{C}$ for both acids, i.e., $K_{\text{aims}} = K_{\text{orgs}} = 1.75 \times 10^{-5} \text{ mol L}^{-1}$ (Fu, 1999), using a temperature regulating factor, f_{acid} (Eqs. 5–6).
 153 The function form for parameterizing f_{acid} (Eq. 7) was adapted from Li (2016). The molar concentrations of the acids and H^+
 154 in the soil water are calculated using Eqs. 8–10. In these equations, 10^{-4} is a dimension adaptor (for each 3-hour time step), h
 155 denotes the thickness of each soil layer (m), SM stands for the soil moisture in volumetric water content ($\text{m}^3 \text{ m}^{-3}$), M_{ami} and
 156 M_{org} represent the average molar mass of amino acids (128 g mol^{-1}) and the other organic acids (119 g mol^{-1}), respectively,

157 in root exudates (Fu, 1999), a_{ami} and a_{org} are the mass fractions of the two categories of acids in root exudates
 158 (dimensionless), Ex is the root exudates in the soil layer (kg ha^{-1}) and sph' denotes the soil pH, and $c_{\text{H}(\text{soil})}$ is the H^+
 159 concentration corresponding to the most lastly updated pH. At each time step (3 h) of the model simulation, 6% of the net
 160 primary productivity is assumed to be released into the soil profile via root exudation. This assumption was made by
 161 referring to the experimental data of some other tree species (Miao, 2015). The Ex in the soil layer is determined by
 162 portioning the exudate quantity according to the vertical distribution of the root biomass in the soil profile of root depth.

$$\Delta[\text{H}^+]_{\text{ex}} = \Delta[\text{H}^+]_{\text{ami}} + \Delta[\text{H}^+]_{\text{org}} \quad (2)$$

$$K_{\text{ami}} = \Delta[\text{H}^+]_{\text{ami}} (c_{\text{H}(\text{soil})} + \Delta[\text{H}^+]_{\text{ami}})(c_{\text{ami}} - \Delta[\text{H}^+]_{\text{ami}})^{-1} \quad (3)$$

$$K_{\text{org}} = \Delta[\text{H}^+]_{\text{org}} (c_{\text{H}(\text{soil})} + \Delta[\text{H}^+]_{\text{org}})(c_{\text{org}} - \Delta[\text{H}^+]_{\text{org}})^{-1} \quad (4)$$

$$K_{\text{ami}} = K_{\text{amis}}f_{\text{acid}} \quad (5)$$

$$K_{\text{org}} = K_{\text{orgs}}f_{\text{acid}} \quad (6)$$

$$f_{\text{acid}} = 0.81 + 0.0077T \quad (7)$$

$$c_{\text{ami}} = 10^{-4}h^{-1}\text{SM}^{-1}M_{\text{ami}}^{-1}a_{\text{ami}}\text{Ex} \quad (8)$$

$$c_{\text{org}} = 10^{-4}h^{-1}\text{SM}^{-1}M_{\text{org}}^{-1}a_{\text{org}}\text{Ex} \quad (9)$$

$$c_{\text{H}(\text{soil})} = 10^{-\text{sph}'} \quad (10)$$

163 According to Rxn 2, the H^+ concentration changes due to the hydrolysis of Al^{3+} derived from decomposition of tea
 164 plant residues ($\Delta[\text{H}^+]_{\text{res}}$) are calculated by solving the equation (numerical method by Newton iteration) of Eq. 11. In this
 165 equation, K_w ($(\text{mol L}^{-1})^2$) and K_b ($(\text{mol L}^{-1})^3$) denote the water dissociation constant and ionization equilibrium constant of
 166 aluminum hydroxide ($\text{Al}(\text{OH})_3$), respectively, and $c_{\text{Al(III)}}$ is the molar concentration of Al^{3+} in the soil water (mol L^{-1}). As
 167 both water dissociation and $\text{Al}(\text{OH})_3$ ionization are also thermodynamic processes, their equilibrium constants
 168 (dimensionless) vary with soil temperature and are thus determined following Eqs. 12–13, wherein the values at 25 °C, i.e.,
 169 $K_{\text{ws}} = 1 \times 10^{-14} (\text{mol L}^{-1})^2$ and $K_{\text{bs}} = 1.3 \times 10^{-33} (\text{mol L}^{-1})^3$ for water and $\text{Al}(\text{OH})_3$, respectively (Fu, 1999), are corrected by the
 170 factors f_w and f_b , respectively. The parameterization for f_w (Eq. 14) was cited from Li (2016), and f_b was parameterized by Eq.
 171 15. For calculation of $c_{\text{Al(III)}}$ in Eq. 16, M_{Al} denotes the molar mass of Al^{3+} (27 g mol^{-1}), b the fraction of hydrolyzed $\text{Al}(\text{OH})_3$
 172 (dimensionless), c the Al content in tea residues (kg kg^{-1} dry matter), and Res the quantity of tea residues in dry matter (kg
 173 ha^{-1}). As the Al concentration in tea leaves varied from 1.2 to 2.7 mg g^{-1} dry matter, the c value was set as $2.3 \times 10^{-3} \text{ kg kg}^{-1}$
 174 dry matter (Hajiboland et al., 2015; Xu et al., 2006).

$$K_w^3 K_b^{-1} = \Delta[\text{H}^+]_{\text{res}}(c_{\text{H}(\text{soil})} + \Delta[\text{H}^+]_{\text{res}})^3(c_{\text{Al(III)}} - \Delta[\text{H}^+]_{\text{res}}/3)^{-1} \quad (11)$$

$$K_w = K_{\text{ws}}f_w \quad (12)$$

$$K_b = K_{\text{bs}}f_b \quad (13)$$

$$f_w = 0.1945e^{0.0645T} \quad (14)$$

$$f_b = 1.09 - 0.0037T \quad (15)$$

$$c_{\text{Al(III)}} = 10^{-4} h^{-1} \text{SM}^{-1} M_{\text{Al}}^{-1} b c \text{Res} \quad (16)$$

175 Using the H^+ concentration changes calculated above, the soil pH most lastly modified by the originally existing
 176 processes, or at the last time step of simulation, is further updated by Eq. 17. The soil pH updated by Eq. 17 is used to update
 177 the independent variable of Eq. 1 so as to provide an update of f_{sph} .

$$\text{sph} = -\lg(c_{\text{H(soil)}} + \Delta[\text{H}^+]_{\text{ex}} + \Delta[\text{H}^+]_{\text{res}}) \quad (17)$$

178 For the processes newly added above, the unknown parameters, a_{ami} , a_{org} and b , were calibrated in this study using the
 179 observed soil pH in the T08 and T12 plots. The independent variables of T , h , SM , and Res , as well as the net primary
 180 production and the root biomass distribution in the soil profile required to calculate Ex , are provided by the model
 181 simulations at each time step.

182 The soil pH dynamics affected by the urea hydrolysis, soil buffering and manure application have already been
 183 considered in the original CNMM-DNDC (Table S3). The CNMM-DNDC with and without the above modifications is
 184 hereafter referred to as the original and modified model, respectively.

185 2.3 Evaluation of model simulations for emissions of both gases

186 The model performances in simulating N_2O and NO emissions from the tea plantations were evaluated by comparing
 187 the simulations of the original and modified models with the field observations. The required input of hourly meteorological
 188 data (air temperature, precipitation, wind speed, solar radiation, humidity) for years with gas flux measurements (2012–2014)
 189 were obtained from the meteorological station at the field site, while those in 2008–2011 were adapted from the daily data at
 190 the nearby government meteorological station (provided by the National Meteorological Information Center:
 191 <http://data.cma.cn/>) by referring to the diurnal patterns of the hourly data observed and provided by the Shennongjia Station
 192 (~40 km south of the tea fields) of the Chinese Ecosystem Research Network. The aforementioned observations were used
 193 for the required inputs of soil properties (SOC, total nitrogen, mass fraction of clay, pH, and bulk density). The required
 194 inputs of field capacity and wilting point (0.38 and 0.16, respectively, in volumetric water content) were calculated by the
 195 pedo-transfer functions used by Li et al. (2019). According to the local survey, the initial biomass of tea seedling
 196 transplanting was set as 1500 kg dry matter (DM) ha^{-1} . The harvest of buds and the trim of canopy were started at the 4th
 197 year after transplanting (YAT), following the local conventional practices. The bud tea was harvested in the T08 from April
 198 to May and August to October in the 4th, 5th and 6th YAT, with annual yields of 37.5–150 kg DM ha^{-1} . The tea plants were
 199 trimmed twice per year in June and November and nearly 40% of the aboveground biomass was cut and left on the ground.
 200 The detailed management practices during the gas measurement period were obtained from Yao et al. (2015, 2018), which
 201 were also adopted during the remaining period of simulation. The simulated soil profile (0–100 cm depth) was divided into
 202 20 layers. The thickness of each layer was 1, 5 and 10 cm for the top 10, middle 2, and other 8 layers, respectively. The time
 203 step of simulation was set as 3 hours. The measured data (Yao et al., 2015, 2018) used for evaluating the model performance

204 included the topsoil temperature and moisture and, the daily fluxes of N₂O and NO emissions from the T08-NN, T08-UN,
 205 and T08-OM in 2012–2014 and, the T12-NN, T12-UN, and T12-OM in 2013–2014 (Figure 1).

206 **2.4 Investigation of fertilization and stand age effects on emissions of both gases**

207 In the field cases involved in this study, the short-term replacement of urea with oilcake was implemented in the 2nd
 208 (T12) or 5th–6th (T08) YAT following the land use change from long-term paddy rice cultivation to perennial tea plantation.
 209 Based on the field observations of N₂O and NO emissions reported by Yao et al. (2015, 2018), the performance of the
 210 original and modified models in simulating the effects of the urea replacement by oilcake was examined through the
 211 comparison between the model relative bias (MRB) magnitudes and the observational error indicated by the coefficient of
 212 variation (CV). An absolute MRB (|MRB|) smaller than the two times CV of the spatially replicated observations, which
 213 represented the observational uncertainty at the 95% confidence interval (CI), was considered to indicate a statistically
 214 satisfactory performance (Dubache et al., 2019). For this examination, the urea replacement effects (E_{ur} , in %) on the N₂O
 215 and NO emissions and their relative observational errors (ε_{ur} , in %) at the 95% CI were calculated using Eqs. 18–19. In both
 216 equations, \overline{E}_o and \overline{E}_u (in kg N ha⁻¹ yr⁻¹) denote the mean annual emission of N₂O or NO from the OM and UN treatments,
 217 respectively, and δ_o and δ_u (in kg N ha⁻¹ yr⁻¹) signify the corresponding observational errors in two times standard deviation
 218 (SD). Equation 19 is analytically established according to Eq. 18 and following the general error propagation theory. The
 219 observed data were directly cited or adapted from Yao et al. (2015, 2018).

$$E_{ur} = 100(\overline{E}_o/\overline{E}_u - 1) \quad (18)$$

$$\varepsilon_{ur} = 100(\overline{E}_u^{-2}\delta_o^2 + (\overline{E}_o^2\overline{E}_u^{-4}\delta_u^2)^{1/2}/(\overline{E}_o/\overline{E}_u - 1)) \quad (19)$$

220 The virtual experiments were designed to evaluate the performance of the original and modified models in simulating
 221 the annual EF_ds and to investigate the effects of fertilizer nitrogen doses on EF_ds. For each field treatment exclusively
 222 applied with urea or oilcake in 2013 or 2014, virtual experiments against nitrogen addition rates varying from zero to 600
 223 (with an interval of 50) kg N ha⁻¹ yr⁻¹ were carried out. For each treatment, the gradient nitrogen doses were set only in the
 224 experimental year but remained at 450 kg N ha⁻¹ yr⁻¹ in the other year(s). The annual EF_ds (the fraction of the increased
 225 fertilizer nitrogen input released in the form of N₂O or NO within the one-year period after fertilization) in percentage for the
 226 nitrogen dose gradients were simulated at each gradient with an interval (N_{50}) of 50 kg N ha⁻¹ yr⁻¹, following Eq. 20,
 227 wherein E_{50+} and E_{50-} denote the simulated annual emissions of N₂O or NO at the higher and lower fertilizer nitrogen dose of
 228 the gradient, respectively.

$$EF_d = 100(E_{50+} - E_{50-})/N_{50} \quad (20)$$

229 The stand age effects on annual N₂O and NO emissions in the early stage (1–6 years) or a full tea plant lifetime (35
 230 years) of a plantation can be investigated if the applicability of the model was proven using available observations at the
 231 field site. Acceptable model applicability can be indicated by a smaller average |MRB| than two times CV of the spatially
 232 replicated observations. The effects of the stand ages during the early stage (1st to 6th YAT) or the full tea lifetime (usually
 233 until approximately the 35th YAT in the region) can be investigated using a virtual experiment. The tea plantation in this

234 virtual experiment was purely fertilized with urea at the conventional timings and doses. Any influencing factor other than
235 stand age should be excluded from this virtual experiment. To ensure the simulations of all the stand ages can be driven by
236 the same meteorological conditions that would be the same as the measured data during the year-round period from
237 September 17th, 2013 to October 9th, 2014, 35 independent scenarios were designed. Thus, the seedling transplanting for the
238 stand ages of 35, 34, ..., 1 year were set to occur in March of 1979, 1980, ..., and 2013, respectively. The field management
239 practices for T08-UN would be set for each stand age scenario.

240 **2.5 Statistics and method to quantify uncertainties**

241 The statistical criteria used in this study to evaluate the model performance include (i) the index of agreement (IA), (ii)
242 the Nash-Sutcliffe index (NSI), (iii) the determination coefficient (R^2) and slope of the zero-intercept univariate linear
243 regression (ZIR) of the observations against the simulations, and (iv) the MRB. The IA falls between 0 and 1, with a value
244 closer to 1 indicating a better simulation. An NSI value (ranged from minus infinity to 1) between 0 and 1 shows acceptable
245 model performance, whereas closer to 1 is better. Better model performance is indicated by a slope and an R^2 value that is
246 closer to 1 in a significant ZIR. The performance is regarded as acceptable if a significant ZIR with its slope closer to 1 can
247 be obtained or the |MRB| on average is smaller than the two times CV of replicated observations. Akaike information
248 criterion (AIC) is applied to evaluate the significance of the multivariate linear regression. The additional independent
249 variable is significant when the value of AIC decreases. For more details on these criteria, refer to Eqs. S1–5 in Table S4.

250 The model simulation error (ε_s) indicated the simulated bias diverging from the observation. It represented the total
251 simulation uncertainty and was made of the uncertainty due to the model insufficiencies in scientific structure or process
252 parameters ($\varepsilon_{\text{model}}$) and that due to the uncertainties of input items ($\varepsilon_{\text{input}}$) (Zhang et al., 2019). For the investigation of stand
253 age effects, the mean relative ε_s and its random uncertainty (95% CI) for either gas were estimated as the mean and the two
254 times SD of the MRBs relative to the observations for three stand ages (i.e., those in the T12-UN and T08-UN fields in the
255 2nd and 5th–6th YAT). The relative ε_s values for a gas were regarded to be equal among the different stand age scenarios. The
256 mean or the two times SD of the relative ε_s was converted to its absolute magnitude through multiplying it with the product
257 of an adjustment factor and the simulated gas emission quantity. The adjustment factor was obtained from the model
258 validation of the three stand ages, which was estimated as the mean of the ratios of individual observations to simulations.
259 Since the uncertainties of the model input items were known as random errors, the $\varepsilon_{\text{input}}$ was a random error. It was estimated
260 using the Monte Carlo test with Latin hypercube sampling (Helton and Davis, 2003) within the uncertain ranges (95% CI) of
261 sensitive input items, which included the soil properties (bulk density, pH, clay fraction, SOC and soil total nitrogen content)
262 (e.g., Li, 2016), thermal degree days (TDD) for maturity, and nitrogen content in the different plant stages (seedling, early
263 and harvest stages). According to the measurement errors, the uncertain ranges of the input items were 1.11–1.35 g cm⁻³ for
264 bulk density, 5.6–6.4 for pH, 0.120–0.128 for clay fraction, 9.6–13.6 g kg⁻¹ for SOC content, and 1.00–1.48 g kg⁻¹ for total
265 nitrogen content. The uncertainties of the TDD and, plant nitrogen content in the three stages were assumed to be $\pm 5\%$ of
266 the default values, which were 2500 °C, and 7.8, 6.8 and 6.0 g N kg⁻¹ DM, respectively. A uniform distribution for sampling

267 was assumed in the Monte Carlo test, in which the simulations were iterated until the mean of the simulated gas emission
268 quantities for all iterations converged to certain level within the tolerance of 1%. The $\varepsilon_{\text{input}}$ at the 95% CI was presented as
269 the double SDs of these iterated simulations.

270 If not specified, errors are presented hereafter at the 95% CI.

271 In this study, the statistical analyses and graphical comparisons were performed with the SPSS Statistics Client 19.0
272 (SPSS Inc., Chicago, USA) and Origin 8.0 (OriginLab, Northampton, MA, USA) software packages.

273 **3 Results**

274 **3.1 Calibration of modified model for soil pH simulation**

275 Using the topsoil (0–15 cm) pH (6.0) prior to tea seedling transplanting and the values of 5.4 and 5.0 measured in T12-
276 UN and T08-UN, respectively, in September 2013, each of the three parameters involved in the modified model (Eqs. 8–9
277 and 16) was calibrated to 5.0×10^{-4} for a_{ami} and a_{org} , and 1.0×10^{-3} for b , respectively. The simulations of the modified
278 CNMM-DNDC with these calibrated parameters resulted in topsoil (0–15 cm) pH values of 5.42 and 5.01 in the T12-UN
279 and T08-UN fields, respectively, in September 2013, which were consistent with the observations. Differently, the soil pH
280 simulated by the original model remained nearly constant (approximately 6.0) during the 6-year period, despite the transient
281 increases due to urea hydrolysis. Nevertheless, it is still required to validate the simulations of the modified model on the soil
282 pH changes due to tea growth using more field observations under different conditions.

283 **3.2 Model validation for soil environment and emissions of both gases**

284 Both the original and modified models accurately predicted the seasonal dynamics and magnitudes of topsoil
285 temperature and moisture (Figures 1a–b). The satisfactory model performance was indicated by the statistics in Table 1.

286 The measured daily N_2O and NO fluxes were highly variable across the entire observation period (Figures 1c–n). The
287 original and modified models generally captured the seasonal patterns of both gases for different field treatments, even
288 though the magnitudes of some peak fluxes were inconsistent with the observations. In comparison, the original model
289 generally overestimated the peak emissions of both gases. The performance of both models was similar and satisfying for the
290 daily fluxes as indicated by the comparably IA, NSI, and ZIR slope and R^2 values (Table 1). For the original model, three
291 (NO) and five (N_2O) of the nine individual simulations for each gas showed |MRBs| larger than the corresponding observed
292 two times CV, while |MRBs| larger than the observed two times CV were four (NO and N_2O) for the modified model (Table
293 S5). However, the statistics of both models still indicated agreements for annual emissions, with the IA and NSI values of
294 0.96–0.98 and 0.81–0.94, respectively, for N_2O and NO (Table 1). In addition, the modified model improved the simulation
295 of annual N_2O emission, with higher IA, NSI, ZIR slope and R^2 values of 0.98, 0.94, 0.97 and 0.94 ($p < 0.001$), respectively
296 (Table 1, Figure 2). These results indicate that the modified CNMM-DNDC can effectively simulate the daily and annual
297 emissions of both gases from the tested tea plantations. Additionally, the modified model resulted in adjustment factors of

298 0.86 and 1.09 and relative ε_s values of $17 \pm 20\%$ and $-8 \pm 14\%$ for the annual N_2O and NO emissions from the UN
299 treatments and adjustment factors of 1.00 and 0.97 and relative ε_s values of $0.2 \pm 24\%$ and $6 \pm 38\%$ for the N_2O and NO
300 emissions from the OM plots, respectively. These adjustment factors and relative ε_s were used to estimate the absolute total
301 errors of the simulated emissions.

302 **3.3 Effects of organic fertilization on emissions of both gases**

303 According to the field observations, the short-term replacement of urea by oilcake stimulated the annual N_2O
304 emissions by $\sim 62\%$ (ranging between 35–95% or $5.3\text{--}13.7 \text{ kg N ha}^{-1} \text{ yr}^{-1}$) but simultaneously mitigated the annual NO
305 emissions by $\sim 25\%$ (ranging between 12–33% or $2.4\text{--}6.0 \text{ kg N ha}^{-1} \text{ yr}^{-1}$). Based on the statistical analysis using linear mixed
306 models, both the stimulation and mitigation effects were significant ($p < 0.05$) (Yao et al., 2015). The average relative
307 observational errors of these effects were $\sim 97\%$ (ranging between 92–106%) for N_2O and $\sim 73\%$ (ranging between 60–83%)
308 for NO (adapted from Yao et al., 2015, 2018; Table S6). The simulated effects of the fertilizer replacement on annual N_2O
309 emissions by the modified model showed stimulations by $\sim 36\%$ (ranging between 24–49% or $5.7\text{--}9.1 \text{ kg N ha}^{-1} \text{ yr}^{-1}$), with
310 |MRB| of $\sim 36\%$ (ranging between 4–56%) (Table S6). The |MRB| magnitudes were significantly lower than the relative
311 observational errors ($p = 0.02$), indicating consistency between the simulated and observed effects. The inhibition effects of
312 the fertilizer replacement on annual NO emissions were about 14% (varying between 1–21% or $0.1\text{--}4.1 \text{ kg N ha}^{-1} \text{ yr}^{-1}$) by
313 the modified model except for some underestimation, which indicated the consistent effects between the simulations and
314 observations (Table S6). As these results suggest, the model with improvements in scientific processes could simulate the
315 effects of short-term replacement of urea by oilcake on N_2O and NO emissions in the early stage of the new tea plantations.

316 **3.4 Nitrogen dose effects on annual direct emission factors of both gases**

317 As Figures 3a–b and S1a–b show, the simulated annual emissions of either gas non-linearly varied with the nitrogen
318 addition rate in form of urea or oilcake. Accordingly, for the modified model, the simulated annual $\text{EF}_{\text{d,s}}$ of either gas at
319 different levels of fertilizer doses increased linearly with the urea addition rates (Figures 3c–d) but nonlinearly with the
320 organic manure addition rates (Figures 3e–f). In comparison with the linear fittings for the manure treatment, the
321 relationships were better fitted the non-linear curves, as indicated by the decreased AIC values (1.74 versus 1.72 for N_2O and
322 0.53 versus 0.31 for NO). The simulations by the original model showed similar results with those of the modified model
323 (Figures 3c–f and S1c–f). The original and modified model simulations of annual gas emissions for the two experimental
324 nitrogen doses (zero and $450 \text{ kg N ha}^{-1} \text{ yr}^{-1}$) resulted in significantly consistent $\text{EF}_{\text{d,s}}$ with the field observations for N_2O
325 (Figure 4a). In comparison with the original model, the modified model performed better in simulating the $\text{EF}_{\text{d,s}}$ of N_2O ,
326 increasing IA from 0.78 to 0.89 and NSI from 0.10 to 0.64 (Table 1). For NO, the simulated annual $\text{EF}_{\text{d,s}}$ by both models
327 tended to be positively related with the field observations (Figure 4b), with acceptable IA of 0.85–0.89 and NSI of 0.38–0.50
328 (Table 1). These results imply that, compared with the original model, the modified version with the pH reduction processes
329 added in this study could be applied to simulate the $\text{EF}_{\text{d,s}}$ of either gas from tea plantations under different field conditions.

330 3.5 Effects of stand ages on emissions of both gases

331 The measured annual N₂O and NO emissions from the T12-UN and T08-UN fields in the 2nd and 5th–6th year ranged
332 from 14.4–21.1 and 13.1–19.4 kg N ha⁻¹ yr⁻¹, with double CVs of ~43% (ranging from 9–72%) and ~13% (ranging from
333 6–21%), respectively (Yao et al., 2015, 2018). The original model simulations of annual N₂O and NO emissions showed
334 |MRB| of ~33% (ranging from 6–76%) and ~6% (ranging from 3–10%) respectively, while |MRBs| of the annual N₂O and
335 NO emissions were ~17% (ranging from 11–28%) and ~8% (ranging from 1–14%) for the modified model. The |MRB| on
336 average for either gas (by both models) was smaller than the two times CV on average in the observations. This evaluation
337 indicates that the modified model with the new processes could also reliably simulate the emissions of both gases under
338 different stand ages and therefore be applicable for investigating stand age effects in long time using a virtual experiment.

339 For the modified model, the simulated daily topsoil (0–15 cm) pH during the early 6-year period basally declined
340 gradually, with a temporary sudden pulse immediately following the urea application events either in spring or autumn
341 (Figure 5a). Although the simulated pH declined from the initial value of 6.0 to less than 5.0, it was still higher than 4.5
342 which was the threshold set in the model to trigger the chemo-denitrification process. Different from the slightly nonlinear
343 changes in the simulated basal pH, the simulated annual emissions of N₂O and NO gradually increased with the stand ages in
344 the early four or five years, but then decreased gradually. The variation trend for the simulated annual emissions of either gas
345 against the early stand ages (1–6 years) could be fitted by a quadratic polynomial equation instead of the linear relationship
346 as indicated by the decreased AIC values for the non-linear fitting as compared with that for linear regression (–1.75 versus
347 0.66 for N₂O, and –3.67 versus 0.55 for NO). Similar nonlinear relationships were also obtained for the simulations by the
348 original model (Figure S2). As Figure 5 indicated, almost all the field observations in the fertilized fields not only generally
349 fell within the range of the uncertainty induced by the input items, but also within the upper and lower bounds of uncertainty
350 (95% CI) of the regressions. Compared with the uncertainty induced by the inputs ($\varepsilon_{\text{input}}$), the absolute values of the total
351 model uncertainty (ε_s) were much smaller, which only accounted for 32% and 35% of the $\varepsilon_{\text{input}}$ for N₂O and NO, respectively.

352 Although the performances of both models in simulating the emissions of both gases were comparable in early stand
353 ages, the original and modified model thereafter performed quite differently. The 35-year simulations demonstrated that the
354 above polynomial functions derived from the original model simulation applied for both gases during the full tea lifetime;
355 but those derived from the modified model did not apply for the mid to late stand stages (Figure 6a). After the annual
356 emissions of both gases simulated by the modified model reached peak values, they decreased near-linearly until around the
357 15th YAT, when the chemo-denitrification process was triggered by the pH threshold (4.5) set in the model. Thereafter, the
358 emission of either gas gradually increased at a very small annual increment (Figure 6a). Thus, the emissions of both gases
359 simulated by the original model were about two times those by the modified model during the mid to late tea stand ages. The
360 ε_s of the simulation by the modified model were ranged from 2.11 to 2.89 and -1.63 to -0.78 for N₂O and NO, respectively
361 (Figure 6a), indicating the potential overestimation or underestimation of either gas for 35-year simulations. Meanwhile,
362 different from the stable topsoil pH (except for the sudden pulse due to urea hydrolysis) by the original model, the simulated

363 basal pH of 0–15 cm by the modified model continued to decrease, finally reaching 3.74 (Figures 6b–c). In addition, the 35-
364 year simulation showed that the negative effects of soil pH on tea yield increased with the stand ages, resulting in the
365 reduction by 0.3–3.4% (Figure 6d). These results suggest that the modifications by adding the processes regulating soil pH
366 dynamics are necessary for accurately quantifying the long-term emissions of N₂O and NO from tea plantations.

367 **4 Discussion**

368 **4.1 Model modifications**

369 The modified CNMM-DNDC was hypothesized to reflect the general knowledge that tea can grow in soils with a
370 suitable pH within 4.0–6.5 (Cao et al., 2009). But the transient increase of soil pH due to urea hydrolysis has no impact on
371 plant growth, as the soil pH could be recovered within a few days due to soil buffering effect. Due to the lack of observed tea
372 yields, the parameterized impact of soil pH on tea growth could not be calibrated or validated in this study, but virtual
373 experiments showed increased yield reduction with increasing stand age, implicating the intensified negative effects on plant
374 growth for older tea plantations. The newly added scientific processes relating to pH reduction were calibrated using the
375 observed soil pH for different stand ages during the early stage of a tea plantation. Although the simulations showed that the
376 modified CNMM-DNDC with the calibrated parameters could accurately reflect the basal soil pH declination during the
377 early years, validation was still missing due to a lack of available independent observation of pH. However, the studies of the
378 tea plantations in Jiangsu and Anhui provinces showed that the average soil pH (0–20 cm) declination rate was 0.06 pH yr⁻¹
379 (Luo, 2006; Su, 2018). For the simulation of 35-year tea plantation in this study, the calculated average annual soil (0–20 cm)
380 pH declination rate was close to the reports with the value of 0.064. Therefore, the consistent declination rate indicates the
381 modifications improve the scientific mechanisms of the biogeochemical model which could be applied for long time
382 simulation. As the actual soil pH would not decline constantly (Yao et al., 2018), the validation of soil pH dynamics for long
383 time is still necessary. The simulated annual emissions by both models were comparable in the early tea stand ages, but those
384 by the modified model were much lower in the mid to late stages of tea lifetime. According to the modifications, the
385 different annual emissions of both gases should be primarily attributed to the soil pH differences. Therefore, the proper
386 simulation of soil pH declination for long time increased the reliability of the simulated variation of annual emissions even
387 though validation of the differences was still missing due to lacking of field observations. Thus, further study is still needed
388 to confirm the general model applicability, especially for the simulations of long term yields, soil pH dynamics, N₂O and NO
389 emissions from tea plantations subject to different conditions.

390 **4.2 Model performance**

391 This study was the first study testing the original or modified models against the measurements of N₂O and NO
392 emissions from a tea plantation. The results showed that both the original and modified models accurately captured the high

393 temporal variations of daily N₂O and NO emissions driven by the application of fertilizers, stand ages and weather
394 conditions (Yao et al., 2015, 2018). Many previous studies did not report the R^2 of regressions between the observed and
395 simulated daily fluxes of either gas, usually due to poor model performance (Bell et al., 2012; Bouwman et al., 2010;
396 Butterbach-Bahl et al., 2009). Considering the large uncertainties of field measurements as indicated by the SDs of the
397 observations and the complexity of the management practices, the performance of the modified model for either gas was
398 encouraging. Yao et al. (2015, 2018) obtained significant revised “hole-in-pipe” (HIP) regressions for the observed daily
399 N₂O plus NO fluxes as the dependent variable and the soil ammonium plus nitrate concentrations, temperature and moisture
400 as the multiple independent variables. Compared with the R^2 values of the original HIP regressions fitting the daily
401 observations, those of the revised HIP model more than doubled and were up to 0.95–0.97 (Yao et al., 2015, 2018).
402 Similarly, the daily simulations by the modified model also resulted in significant revised HIP regressions that showed more
403 than doubled R^2 (0.48–0.55) in comparison with the values (0.01–0.12) of the original HIP (Mei et al., 2011), despite of the
404 smaller determination coefficients than those for the field observations. The improvements of the revised HIP regression by
405 both observations and simulations were due to the consideration of the temperature- and moisture-regulated effects of
406 nitrogen substrates for both nitrification and denitrification processes that produce N₂O and NO.

407 For the annual N₂O emissions, the statistics of the modified model were all better than the original model, indicating
408 the modifications about soil pH reduction improve the model performance in tea plantations. Thus, the simulated
409 corresponding effects of organic fertilization and EF_{d,s} by the modified model were more consistent with the observations.
410 However, the simulated annual NO emissions by the modified model were not much improved in comparison with those by
411 the original model. The underestimation (2.56 kg N ha⁻¹ yr⁻¹) and overestimation (3.29 kg N ha⁻¹ yr⁻¹) of the NO emission in
412 2014 for T08-UN and T08-OM, respectively, resulted in the significant underestimation of the inhibition effects and
413 increased model relative bias for the modified model. The inhibited NO emissions were also partly attributed to the soil
414 heterotrophic nitrification (Yao et al., 2015), which is the direct oxidation of organic nitrogen to nitrate without passing
415 through mineralization. However, the heterotrophic nitrification was not considered in the model, which may result in the
416 overestimated NO emissions in 2014 for the manure treatments by both models. In addition, compared with the original
417 model, the underestimated NO emission mentioned above was also the key reason for the unsatisfactory simulation of EF_{d,s},
418 which led to the increment of the ZIR slope by 8% (1.0 for the ZIR without T08-UN and 1.08 for the ZIR with T08-UN).
419 Therefore, further study is still required for validating the model performance in simulating NO emissions under different
420 fertilization conditions.

421 **4.3 Contribution of the dominant process for emissions of both gases**

422 The CNMM-DNDC model simulates the emissions of N₂O and NO from nitrification and denitrification separately,
423 and then sums them up to give the overall emissions of either gas contributed by both processes (e.g., Li, 2016; Zhang et al.,
424 2018). Some researchers have used the NO and N₂O molar ratio levels higher or lower than 1 to indicate nitrification or
425 denitrification as the dominant process for the emissions of either gas (e.g., Yamulki et al., 1995). However, Wang et al.

426 (2013) have indicated that such criteria may not be applicable, as they commonly observed molar ratios greater than 1 under
427 strict anaerobic conditions with low to moderate initial nitrate concentrations in a calcareous soil. This viewpoint could be
428 supported by the simulated major contributions of the denitrification process by both models, accounting for 63–67% and
429 59–62% of the annual N₂O and NO emissions, respectively, for all the fertilized fields. These larger contributions from the
430 denitrification process could be at least partially attributed to the hot and humid climate from April to September, which
431 resulted in favourable soil moisture and thus facilitated the N₂O and NO emissions. This explanation could be supported by
432 the simulated soil moisture and N₂O emissions from the T08-UN treatment with observations in two consecutive full years.
433 The simulated daily soil moisture falling in the range of 60–90% WFPS appeared at a frequency of only 40% during the
434 two-year period. However, the simulated cumulative N₂O emissions (25.7 kg N ha⁻¹) occurring on the days with such
435 relatively high moisture contents accounted for 61% of the total modelled quantity of this gas (42.0 kg N ha⁻¹). It is accepted
436 that nitrification generally dominates N₂O production in soils with less than 60% WFPS (e.g., Chen et al., 2013). The
437 dominant contributions of denitrification to N₂O and NO emissions by the simulations could also be supported by previous
438 experimental/modelling studies (Chen et al., 2017; Zhang et al., 2017). However, direct validation of the simulations by the
439 original/modified model on the contributions of nitrification or denitrification is still lacking, due to no available direct
440 measurement of N₂O or NO emissions from either process. This challenge will need to be overcome in future studies.

441 **4.4 Effects of organic fertilization on emissions of both gases**

442 For the tea plantations, the applied fertilizers and the retained nitrogen in the soil are consumed by plant uptake,
443 microbial processes and physical losses through ammonia volatilization and nitrate leaching (e.g., Zhang et al., 2015).
444 Accordingly, changes in fertilizer types would affect the nitrogen transformation from the fertilizer to those available for the
445 losses, thus altering the N₂O and NO emissions (e.g., Deng et al., 2013; Goulding et al., 2008; Skinner et al., 2014). Organic
446 fertilization has been widely encouraged in tea cultivation since it can reduce synthetic nitrogen inputs into the biosphere
447 while improving both soil fertility and carbon sequestration (e.g., Skinner et al., 2014; Liang et al., 2011; Meng et al., 2005).
448 Yao et al. (2015) observed that short-term replacement of urea with oilcake, which is characterized by a low carbon to
449 nitrogen ratio, stimulated N₂O emissions to a large extent while inhibiting NO releases to a relatively small extent. These
450 observed effects were generally simulated by the original and modified CNMM-DNDC, especially the increased N₂O
451 emissions.

452 According to the model simulations, the stimulated N₂O emissions were jointly attributed to (i) the enhanced
453 production of this gas, as well as nitrate, in promoted nitrification and (ii) the enhanced production of this gas in promoted
454 denitrification. The promoted nitrification was due to less ammonia volatilization derived from the organic nitrogen
455 mineralization than the urea hydrolysis (~1.0 versus 13 kg N ha⁻¹ yr⁻¹). The oilcake mineralization slowly produced
456 ammonium, while the deep placement of the fertilizer also inhibited ammonia volatilization. In comparison, the urea
457 hydrolysis quickly transformed the fertilizer nitrogen form into ammonium within a few days following the fertilization
458 event, when the hydrolysis-derived pulse increase of soil pH (Figure 5a) stimulated ammonium loss by ammonia

459 volatilization. The denitrification was promoted not only by the improved supply of nitrate (as the primary nitrogen substrate)
460 from the promoted nitrification (Figure S3), but also by the enhanced activity of denitrifiers that have a very high affinity for
461 the carbon substrates provided by the organic manure decomposition (e.g., Li et al., 2005; Skinner et al., 2014; Snyder et al.,
462 2009). For the annual NO emissions of the three paired OM-versus-UN cases, the modified model resulted in consistent
463 decrease (1–21%) due to the full urea replacement by oilcake. The simulations showed that 0–44% of the decreases was
464 ascribed to the promoted nitrification (Table S5), whereby more nitrate was produced as the final product but less NO was
465 produced as the by-product. The remaining 56–100% of the decreases, however, was attributed to the promoted
466 denitrification (Table S5), whereby more NO was reduced to N₂O (e.g., Mejjide et al., 2007; Snyder et al., 2009; Vallejo et
467 al., 2006). Regarding the contributions of denitrification to the overall N₂O or NO emissions, the simulations showed no
468 significant effect from the full urea replacement by oilcake. However, validation of this simulated insignificance is still
469 lacking, because no direct observations for the process contributions are currently available. Further study is still needed to
470 validate the model's performance in simulating the contributions of nitrification or denitrification to the emissions of either
471 gas from tea plantations.

472 **4.5 Effects of nitrogen fertilizer doses on direct emission factors of both gases**

473 Validation of the linear or nonlinear relationships for the urea or manure treatments from the virtual experiment was
474 still lacking, since there was no available data from the experimental field site for the multiple fertilizer gradients.
475 Nevertheless, the relationships of the simulated EF_ds against the nitrogen doses suggested that paired field observations of
476 fertilized and unfertilized treatments, or those of two largely different nitrogen addition rates, as used in many field studies
477 (e.g., Yao et al., 2015, 2018), would yield greatly biased EF_ds of either gas from the tea plantations, particularly creating a
478 gross underestimation for moderate to high nitrogen addition rates. This conjecture from the virtual experiment was
479 supported by two studies so far available for field observations of N₂O emissions from tea plantations treated with nitrogen
480 dose gradients (Han et al., 2013 and Hou et al., 2015), even though similar literature support for NO was still lacking. These
481 experimental studies showed that the EF_d determined by the lowest nitrogen addition rates showed 30% underestimation on
482 average as compared with the value by the highest nitrogen inputs (adapted from Han et al., 2013 and Hou et al., 2015).
483 Obviously, this study implicates the potential capacity of the modified CNMM-DNDC as a robust tool to generate EF_ds of
484 tea plantations subject to different conditions, although it is still necessary to widely validate the simulated EF_ds using field
485 observations against multiple gradients of nitrogen fertilizer doses.

486 **4.6 Effects of stand age on emissions of both gases**

487 Relative to the N₂O and NO emissions in the 2nd or 6th YAT, more intensive emissions of both gases were observed in
488 the 5th YAT (Yao et al., 2015, 2018). These relatively intensified emissions were thought to result from the comprehensive
489 effects of increased soil nitrogen and carbon availability for nitrification and denitrification as well as reduced soil pH (Yao
490 et al., 2018). For either gas, the observations in the tea fields either purely applied with urea or oilcake most likely implied a

491 non-linear trend against stand ages with the inter-annual maximum appearing between the 2nd and 5th YAT. This implication
492 was supported by the modified model simulations for a conventionally managed plantation over the full lifetime of tea plant,
493 in which the inter-annual maximum of N₂O emission appeared in the 4th YAT when the initial harvest of tea bud and the first
494 canopy trim occurred. The increases in the early years were mainly ascribed to the increasing root exudates and less-woody
495 residues returning to soil promoted by the tea plant growth. The simulated inter-annual maximum emission of N₂O appeared
496 in the year when basal soil pH reached the threshold of about 5.0. The inhibition effect of pH on microbial growth is
497 intensified when soil pH is less than this threshold (Figure S4). The adopted pH-influencing mechanisms in the model
498 mainly induced the diminished annual emissions of N₂O following the appearance of the peak, because the emissions of N₂O
499 were associated with the microbial production. In addition to the reduced microbial activity due to low pH inhibition, the
500 post-maximum declinations in the annual gas emissions against the stand ages were also attributed to the reduced
501 availabilities of nitrogen substrates for the microbial processes, due to (i) the higher nitrogen demand for the tea growth
502 stimulated by the multiple bud harvests and two trims per year, as well as (ii) the too slow decomposition of woody residues
503 for old tea remaining on the ground surface. However, experimental support is far less sufficient for these explanations on
504 the variations of gas emissions against the stand ages in the early stage or during the full lifetime of tea growth, and thus
505 further studies are still required. In addition, the smaller total model uncertainty, which only accounts for 33% of the
506 uncertainty induced by inputs, indicated that increasing the reliability of the inputs of soil properties and plant growth
507 parameters can improve the model efficiency.

508 The declination of emissions following the peaks of both gases may not continue throughout the entire lifetime of tea
509 growth, as the process of chemo-denitrification would be triggered once the soil pH decreases to 4.5 or lower, thus
510 promoting the emissions of either gas (e.g., Li, 2016; Pilegaard, 2013). Such a conjecture was well supported by the virtual
511 experiment in this study, which demonstrated that the average soil pH (0–15 cm) decreased to the threshold in the 15th YAT
512 and continued to decrease thereafter. In the model, the chemo-denitrification process occurring under the low soil pH (≤ 4.5)
513 is assumed to transform a portion of the NO produced in the microbial nitrification and denitrification processes into N₂O.
514 Before the chemo-denitrification was triggered, the simulated microbial nitrification stably accounted for ~36% of the
515 overall N₂O and ~41% of the overall NO emissions. When the chemo-denitrification occurred, its contributions to the overall
516 simulated N₂O emissions increased from ~4% to ~8% with increasing stand ages, while the microbial nitrification and
517 denitrification accounted for ~34% and ~59%, respectively. However, these results of gas emissions from the virtual
518 experiment still require validation with field experiments in future studies.

519 **5 Conclusions**

520 To fill a gap in the process-oriented biogeochemical model, the Catchment Nutrient Management Model -
521 DeNitrification-DeComposition (CNMM-DNDC), in this study the effects of soil pH on tea growth and the processes that
522 may induce soil pH reduction due to root exudation and residue decomposition during tea growth were added in the model.

523 Using the two-year field measurements in tea plantations at a subtropical site in central China, the original and modified
524 models were evaluated for simulating nitrous oxide (N₂O) and nitric oxide (NO) emissions from this important type of
525 agricultural ecosystem. Both the original and modified models showed comparable performance for simulating the daily and
526 annual emissions of N₂O and NO from the tested tea plantations at the early stage, especially before the initial tea harvest
527 and the first trims. The modified model was further tested through simulating the emissions of both gases affected by short-
528 term replacement of synthetic fertilizer (urea) with organic manure (oilcake), gradient nitrogen doses of the two fertilizers
529 and different stand ages of new tea plantations. Both observations and simulations demonstrated that short-term replacement
530 of urea with oilcake can largely stimulate N₂O emissions and mitigate NO emissions. The simulations by the modified model
531 also showed linear relationships between the direct emission factors (EF_ds) of either gas against the nitrogen doses for tea
532 plantations amended with synthetic fertilizer and non-linear relationship for those plantations applied with organic manure.
533 These relationships supported the hypothesis that paired field observations against two largely different nitrogen addition
534 rates, which have been very often implemented in field studies, lead to significant biases for the measured EF_ds of either gas
535 from the tea plantations. These biases particularly induce significant underestimations for the moderate to high nitrogen
536 doses that are typically applied by farms. The model simulations also showed that annual emissions of either gas increase
537 with stand ages within the early stage of a new tea plantation and then gradually decrease until they slightly increase again
538 due to chemo-denitrification triggered by soil pH lower than 4.5. In conclusion, the modified CNMM-DNDC can reflect the
539 comprehensive influences of weather, soil conditions, plant nitrogen demands, and field management practices, thus showing
540 potential to be a powerful tool for investigating long-term emissions of N₂O and NO from tea plantations under specific field
541 management alternatives at the site or regional scale. Nevertheless, experimental data are yet too scarce to validate the model
542 simulations of long-term soil pH changes and their effects on the emissions and EF_ds of both gases from tea plantations. To
543 improve the robustness of the model for application in various tea plantations, comprehensive validations using simultaneous
544 field observations are still necessary. The validations should not only include the variables involved in this study but also
545 others, such as the emissions of other greenhouse gases (carbon dioxide and methane), volatilization of ammonia,
546 hydrological nitrogen losses by leaching and surface runoff, and temporal changes in the SOC stock, which are urgently
547 required.

548 **Code/Data availability**

549 The model, input and output databases can be obtained from the first author and all the observed data sets used in this study
550 can be available from the co-authors.

551 **Author contributions**

552 Zheng, X. and Zhang, W. contributed to develop the idea and enhance the science of this study. Zhang, W. improved the
553 scientific processes of the model, designed and implemented the model simulations and virtual experiments and prepared the
554 manuscript with contributions from all co-authors. Yao, Z., Liu, C., Wang, R. and Wang, K. designed and carried out the
555 field experiments. Li, S. and Han, S. collected and established the input database for modelling. Zuo, Q. and Shi, J. provided
556 the climate data observed in the field site.

557 **Competing interests**

558 The authors declare that they have no conflict of interest.

559 **Acknowledgement**

560 This study was jointly supported by the National Key R&D Program of China (2016YFD0800103), the National Natural
561 Science Foundation of China (41603075, 40711130636) and the Chinese Academy of Sciences (ZDBS-LY-DQC007).

562 **Reference**

- 563 Bell, M.J., Jones, E., Smith, P., Yeluripati, J., Augustin, J., Juszczak, R., Olejnik, J., Sommer, M.: Simulation of soil nitrogen,
564 nitrous oxide emissions and mitigation scenarios at 3 European cropland sites using the ECOSSE model, *Nutr. Cycl.*
565 *Agroecosyst.*,92, 161–181, 2012
- 566 Bouwman, A. F., Stehfest, E., Vankessel, C.: Nitrous oxide emissions from the nitrogen cycle in arable agriculture:
567 estimation and mitigation. In: Smith K (ed) *Nitrous oxide and climate change*, Earthscan, London, 2010.
- 568 Butterbach-Bahl, K., Kahl, M., Mykhayliv, L., Werner, C., Kiese, R., Li, C.: A European-wide inventory of soil NO
569 emissions using the biogeochemical models DNDC/Forest-DNDC, *Atmos. Environ.*, 43, 1392–1402, 2009.
- 570 Cao, D., Zhang, Q., Xiao, J., and Zong, L.: Localized monitoring of soil acidification rate of tea garden in Jiangsu province,
571 *J. Tea Sci.*, 29, 443–448, 2009 (in Chinese).
- 572 Chen, D., Li, Y., Grace, P., Mosier, A.R.: N₂O emissions from agricultural lands: a synthesis of simulation approaches. *Plant*
573 *Soil*, 309, 169–189, 2008.
- 574 Chen, D., Li, Y., Wang, C., Fu, X., Liu, X., Shen, J., Wang, Y., Xiao, R., Liu, D., and Wu, J.: Measurement and modeling of
575 nitrous and nitric oxide emissions from a tea field in subtropical central China, *Nutr. Cycl. Agroecosyst.*, 107, 157–173,
576 2017.
- 577 Chen, H., Li, X., Hu, F., and Shi, W.: Soil nitrous oxide emissions following crop residue addition: a meta-analysis, *Global*
578 *Change Biol.*, 19, 2956–2964, 2013.
- 579 Deng, J., Zhou, Z., Zheng, X., and Li, C.: Modeling impacts of fertilization alternatives on nitrous oxide and nitric oxide
580 emissions from conventional vegetable fields in southeastern China, *Atmos. Environ.*, 81, 642–650, 2013.
- 581 Dubache, G., Li, S., Zheng, X., Zhang, W., and Deng, J.: Modeling ammonia volatilization following urea application to
582 winter cereal fields in the United Kingdom by improving a biogeochemical model, *Sci. Total Environ.*, 660, 1403–1418,
583 2019.
- 584 Fu, X. C.: *University Chemistry*, Higher Education Press, Beijing, 1999 (in Chinese).
- 585 Fu, X. Q., Li, Y., Su, W. J., Shen, J. L., Xiao, R. L., Tong, C. L., and Wu, J.: Annual dynamics of N₂O emissions from a tea
586 field in southern subtropical China, *Plant Soil Environ.*, 58, 373–378, 2012.
- 587 Goulding, K., Jarvis, S., and Whitmore, A.: Optimizing nutrient management for farm systems, *Philos. Trans. R Soc B* 363,
588 667–680, 2008.
- 589 Haas, E., Klatt, S., Fröhlich, A., Kraft, P., Werner, C., Kiese, R., Grote, R., Breuer, L., and Butterbach-Bahl, K.:
590 LandscapeDNDC: a process model for simulation of biosphere–atmosphere–hydrosphere exchange processes at site
591 and regional scale, *Landscape Ecol.*, 28, 615–636, 2012.
- 592 Hajiboland, R., and Poschenrieder, C.: Localization and compartmentation of Al in the leaves and roots of tea plants, *Phyton*,
593 84, 86–100, 2015.

594 Han, W., Xu, J., Wei, K., Shi, Y., and Ma, L.: Estimation of N₂O emission from tea garden soils, their adjacent vegetable
595 garden and forest soils in eastern China, *Environ. Earth Sci.*, 70, 2495–2500, 2013.

596 Helton, J. C., and Davis, F. J.: Latin hypercube sampling and the propagation of uncertainty in analysis of complex systems,
597 *Reliab. Eng. Syst. Saf.*, 81, 23-69, 2003.

598 Hirono, Y., and Nonaka, K.: Nitrous oxide emissions from green tea fields in Japan: contribution of emissions from soil
599 between rows and soil under the canopy of tea plants, *J. Soil Sci. Plant Nut.*, 58, 384–392, 2012.

600 Hirono, Y., and Nonaka, K.: Effects of application of lime nitrogen and dicyandiamide on nitrous oxide emissions from
601 green tea fields, *J. Soil Sci. Plant Nut.*, 60, 276–285, 2014.

602 Hou, M., Ohkama-Ohtsu, N., Suzuki, S., Tanaka, H., Schmidhalter, U., and Bellingrath-Kimura, S. D.: Nitrous oxide
603 emission from tea soil under different fertilizer managements in Japan, *Catena*, 135, 304–312, 2015.

604 Li, C.: Modeling trace gas emissions from agricultural ecosystems, *Nutr. Cycl. Agroecosyst.*, 58, 259–276, 2000.

605 Li, C., Frohling, S., and Butterbach-Bahl, K.: Carbon sequestration in arable soils is likely to increase nitrous oxide
606 emissions, offsetting reductions in climate radiative forcing, *Clim. Change*, 72, 321–338, 2005.

607 Li, C.: *Biogeochemistry: Scientific Fundamentals and Modelling Approach*, Tsinghua University Press, Beijing, 2016 (in
608 Chinese).

609 Li, S., Zheng, X., Zhang, W., Han, S., Deng, J., Wang, K., Wang, R., Yao, Z., and Liu, C.: Modeling ammonia volatilization
610 following the application of synthetic fertilizers to cultivated uplands with calcareous soils using an improved DNDC
611 biogeochemistry model, *Sci. Total Environ.*, 660, 931–946, 2019.

612 Li, Y., White, R., Chen, D., Zhang, J., Li, B., Zhang, Y., Huang, Y., Edis, R.: A spatially referenced water and nitrogen
613 management model (WNMM) for (irrigated) intensive cropping systems in the North China Plain. *Ecol. Model.*, 203,
614 395-423, 2007.

615 Li, Y., Zheng, X., Fu, X., and Wu, Y.: Is green tea still ‘green’?, *Geo: Geography and Environment*, 3, e00021, 2016.

616 Liang, B., Yang, X., He, X., Murphy, D. V., and Zhou, J.: Long-term combined application of manure and NPK fertilizers
617 influenced nitrogen retention and stabilization of organic C in Loess soil, *Plant Soil*, 353, 249–260, 2011.

618 Lin, T., and Yang, X.: The absorption and accumulation characteristics of aluminum in *Camellia Sinensis* and its safety
619 evaluation of drinking tea, *Tea Sci. Tech.*, 4, 1–4, 2014.

620 Luo, M.: Study on soil acidification status and influence factors of tea plantations in Jiangsu province, Dissertation, Nanjing
621 Agricultural University, 2006.

622 Matsumoto, H., Hirasawa, E., Morimura, S., Takahashi, E.: Localization of aluminum in tea leaves. *Plant Cell Physiol.*, 17,
623 627–631, 1976.

624 Mei, B., Zheng, X., Xie, B., Dong, H., Yao, Z., Liu, C., Zhou, Z., Wang, R., Deng, J., and Zhu, J.: Characteristics of
625 multiple-year nitrous oxide emissions from conventional vegetable fields in southeastern China, *J. Geophys. Res.*, 116,
626 D12113.

627 Meijide, A., D éz, J. A., S ánchez-Mart ín, L., L ópez-Fern ández, S., and Vallejo, A.: Nitrogen oxide emissions from an
628 irrigated maize crop amended with treated pig slurries and composts in a Mediterranean climate, *Agr. Ecosyst. Environ.*,
629 121, 383–394, 2007.

630 Meng, L., Ding, W., and Cai, Z.: Long-term application of organic manure and nitrogen fertilizer on N₂O emissions, soil
631 quality and crop production in a sandy loam soil, *Soil Biol. Biochem.*, 37, 2037–2045, 2005.

632 Miao, X.: Effect of tea root secretion on the transformation mechnism of phophorus and aluminum forms in the soil
633 (Dissertation), Huna Agricultural University, 2015 (in Chinese).

634 Morita, A., Yanagisawa, O., Takatsu, S., Maeda, S., Hiradate, S.: Mechanism for the detoxification of aluminum in roots of
635 tea plant (*Camellia sinensis* (L.) Kuntze). *Phytochemistry*, 69, 147–153, 2008.

636 Pang, X.: Effects of tea pruning and polyhoenols on organic acids secretion from roots and mineral contents in *camellia*
637 *sinensis* (Dissertaiton), Nanjing Agricultural Univeristy, 2014 (in Chinese).

638 Pilegaard, K.: Processes regulating nitric oxide emissions from soils, *Philos. Trans. R Soc B* 368, 20130126, 2013.

639 Skinner, C., Gattinger, A., Muller, A., Mader, P., Fliebetabach, A., Stolze, M., Ruser, R., and Niggli, U.: Greenhouse gas
640 fluxes from agricultural soils under organic and non-organic management-a global meta-analysis, *Sci. Total Environ.*,
641 468–469, 553–563, 2014.

642 Snyder, C. S., Bruulsema, T. W., Jensen, T. L., and Fixen, P. E.: Review of greenhouse gas emissions from crop production
643 systems and fertilizer management effects, *Agr. Ecosyst. Environ.*, 133, 247–266, 2009.

644 Su, Y.: Study on soil acidification characteristics and regulation mechanism of tea garderns in southern Anhui province,
645 Dissertaion, Zhejiang University, 2018.

646 Taylor, G.J.: Current views of the aluminum stress response: the physiological basis of tolerance. *Curr. Top. Plant Biochem.*
647 *Physiol.*, 10, 57–93, 1991.

648 Tokuda, S., and Hayatsu, M.: Nitrous oxide flux from a tea field amended with a large amount of nitrogen fertilizer and soil
649 environmental factors controlling the flux, *J. Soil Sci. Plant Nut.*, 50, 365–374, 2004.

650 Vallejo, A., Skiba, U., Garciatorres, L., Arce, A., Lopezfernandez, S., and Sanchezmartin, L.: Nitrogen oxides emission from
651 soils bearing a potato crop as influenced by fertilization with treated pig slurries and composts, *Soil Biol. Biochem.*, 38,
652 2782–2793, 2006.

653 Wang, R., Feng, Q., Liao, T., Zheng, X., Butterbach-Bahl, K., Zhang, W., and Jin, C.: Effects of nitrate concentration on the
654 denitrification potential of a calcic cambisol and its fractions of N₂, N₂O and NO, *Plant Soil*, 363, 175–189, 2013.

655 Xu, C., Yu, G., Sun, D., and Wan, G.: Aluminum content determination in brick-tea with chrome azurol S
656 spectrophotometric method, *Chin. J. Endemiol.*, 25(6), 703–704, 2006.

657 Xue, H., Ren, X., Li, S., Wu, X., Cheng, H., Xu, B., Gu, B., Yang, G., Peng, C., Ge, Y., and Chang, J.: Assessment of
658 private economic benefits and positive environmental externalities of tea plantation in China, *Environ. Monit. Assess.*,
659 185, 8501–8516, 2013.

660 Yamamoto, A., Akiyama, H., Naokawa, T., Miyakazi, Y., Honda, Y., Sano, Y., Nakajima, Y., and Yagi, K.: Lime-nitrogen
661 application affects nitrification, denitrification, and N₂O emission in an acidic tea soil, *Biol. Fertil. Soils*, 50, 53–62,
662 2014.

663 Yamulki, S., Goulding, K.W.T., Webster, C.P., Harrison, R.M.: Studies on NO and N₂O fluxes from a wheat field. *Atmos.*
664 *Environ.* 29, 1627–1635, 1995.

665 Yao, Z., Wei, Y., Liu, C., Zheng, X., and Xie, B.: Organically fertilized tea plantation stimulates N₂O emissions and lowers
666 NO fluxes in subtropical China, *Biogeosciences*, 12, 5915–5928, 2015.

667 Yao, Z., Zheng, X., Liu, C., Wang, R., and Butterbach-Bahl, K.: Stand age amplifies greenhouse gas and NO releases
668 following conversion of rice paddy to tea plantations in subtropical China, *Agr. Forest. Meteorol.*, 248, 386–396, 2018.

669 Zhang, W., Liu, C., Zheng, X., Zhou, Z., Cui, F., Zhu, B., Haas, E., Klatt, S., Butterbach-Bahl, K., and Kiese, R.:
670 Comparison of the DNDC, LandscapeDNDC and IAP-N-GAS models for simulating nitrous oxide and nitric oxide
671 emissions from the winter wheat–summer maize rotation system, *Agric. Syst.*, 140, 1–10, 2015.

672 Zhang, W., Li, Y., Zhu, B., Zheng, X., Liu, C., Tang, J., Su, F., Zhang, C., Ju, X., and Deng, J.: A process-oriented hydro-
673 biogeochemical model enabling simulation of gaseous carbon and nitrogen emissions and hydrologic nitrogen losses
674 from a subtropical catchment, *Sci. Total Environ.*, 616–617, 305–317, 2018.

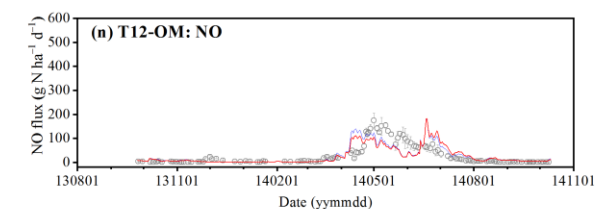
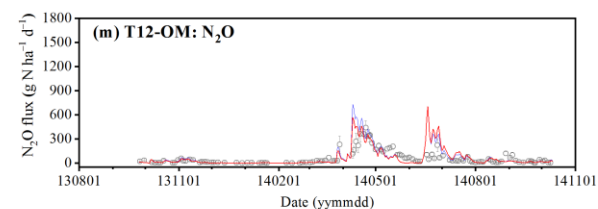
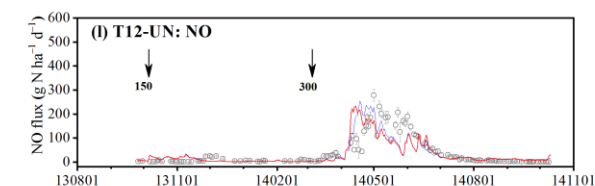
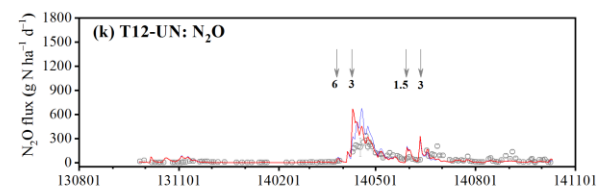
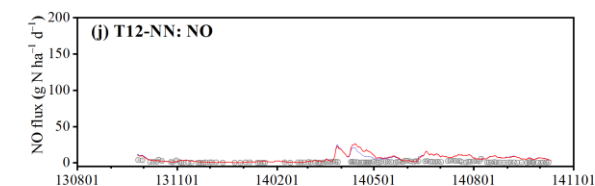
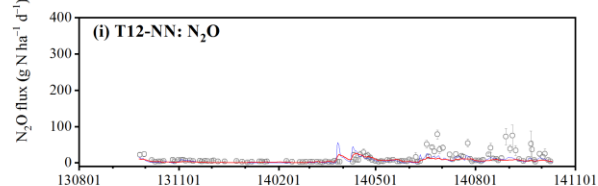
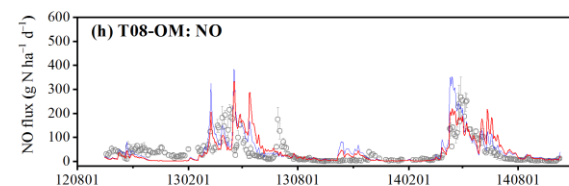
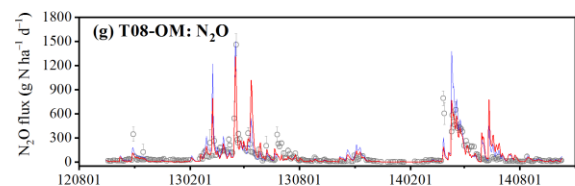
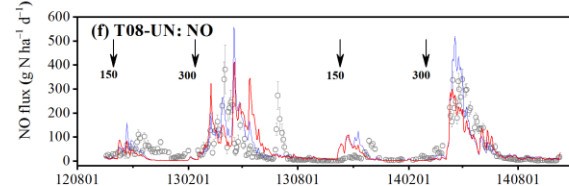
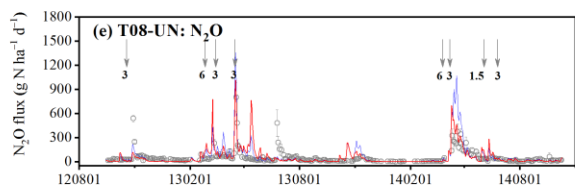
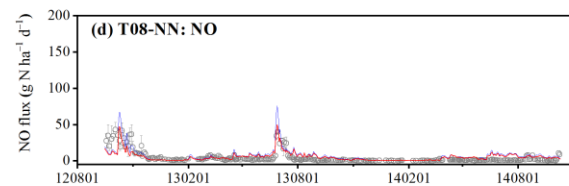
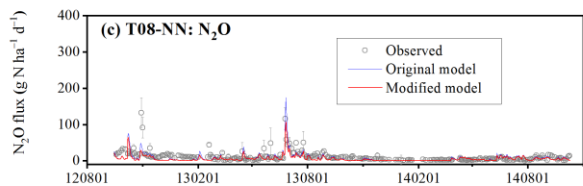
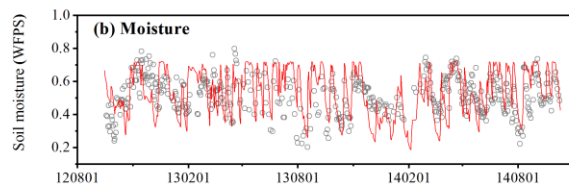
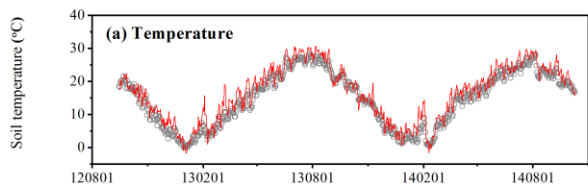
675 Zhang, W., Liu, C., Zheng, X., Wang, K., Cui, F., Wang, R., Li, S., Yao, Z. and Zhu, J.: Using a modified DNDC
676 biogeochemical model to optimize field management of a multi-crop (cotton, wheat and maize) system: a site-scale case
677 study in northern China. *Biogeosciences*, 16, 2905-2922, 2019.

678 Zhang, Y., Zhao, W., Zhang, J., and Cai, Z.: N₂O production pathways relate to land use type in acidic soils in subtropical
679 China, *J. Soil Sediment*, 17, 306–314, 2017.

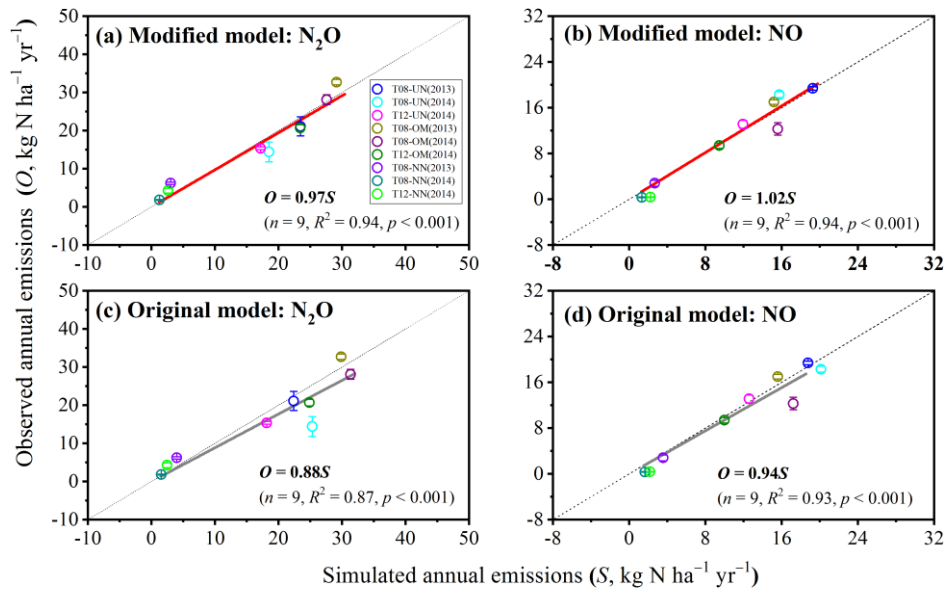
680 Table 1 Statistical evaluation of the original (Ori) and modified (Mod) simulations on the soil temperature (ST), soil moisture (SM), nitrous oxide
 681 (N_2O) and nitric oxide (NO) fluxes as daily means, annual emissions, and annual direct emission factor.

Variable	n	Mean observed	Mean simulated		IA		NSI		Slope		R^2	
			Ori	Mod	Ori	Mod	Ori	Mod	Ori	Mod	Ori	Mod
ST	756	14.8	16.4	16.4	0.98	0.98	0.92	0.92	0.91	0.91	0.95	0.95
SM	504	0.51	0.54	0.54	0.71	0.71	-0.27	-0.27	0.93	0.93	-	-
Daily N_2O	1107	49.5	46.9	42.9	0.82	0.80	0.10	0.18	0.58	0.63	0.51	0.42
Daily NO	1107	31.2	29.8	27.4	0.84	0.80	0.32	0.33	0.68	0.74	0.51	0.41
Annual N_2O	9	16.1	17.8	16.3	0.96	0.98	0.81	0.94	0.88	0.97	0.87	0.94
Annual NO	9	10.3	11.3	10.4	0.98	0.98	0.92	0.94	0.94	1.02	0.93	0.94
EF_{ds} of N_2O	6	3.99	5.03	4.65	0.78	0.89	0.10	0.64	0.81	0.88	0.63	0.80
EF_{ds} of NO	6	3.05	2.95	2.77	0.89	0.85	0.50	0.38	1.01	1.08	0.50	0.51

682 n , number of data pairs. For definitions of IA, NSI, Slope and R^2 , refer to Subsection 2.5 in the text.

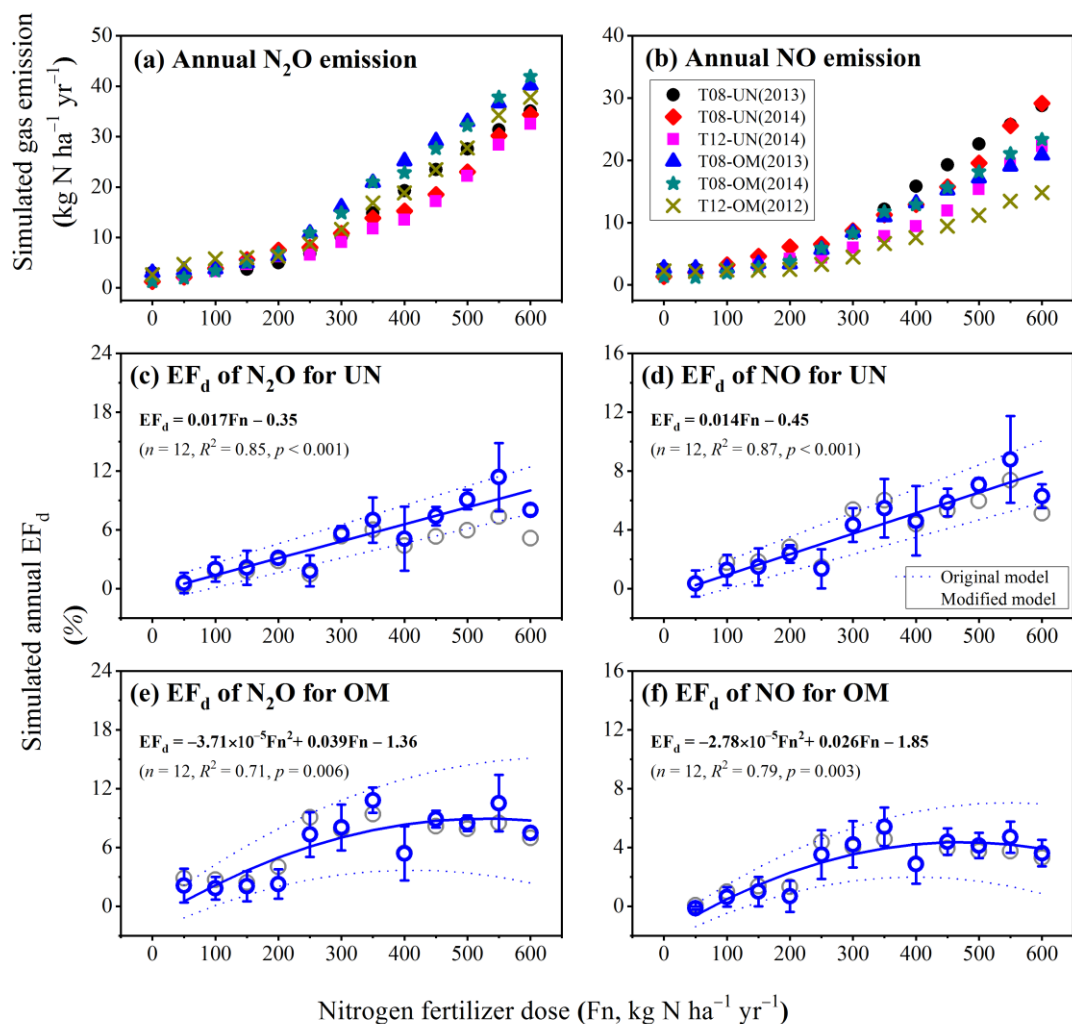


684 **Figure 1: Observed and simulated daily mean soil (5 cm) temperature, soil (0–6 cm) moisture, nitrous oxide (N₂O) and nitric oxide**
685 **(NO) fluxes from tea fields of different treatments by the original and modified models. T08 and T12 represent the fields with tea**
686 **seedling transplanting in 2008 and 2012, respectively. NN, UN and OM encode the no nitrogen applied, and fertilization with urea**
687 **and oilcake, respectively. The grey- and black-line arrows indicate the dates of irrigation and fertilization, respectively. The**
688 **number stands for the applied water amount in cm or fertilizer dose in kg N ha⁻¹. The vertical bar for each observation in panels**
689 **c–n indicates the standard error of four spatial replicates. The legends in panel c apply for all panels.**



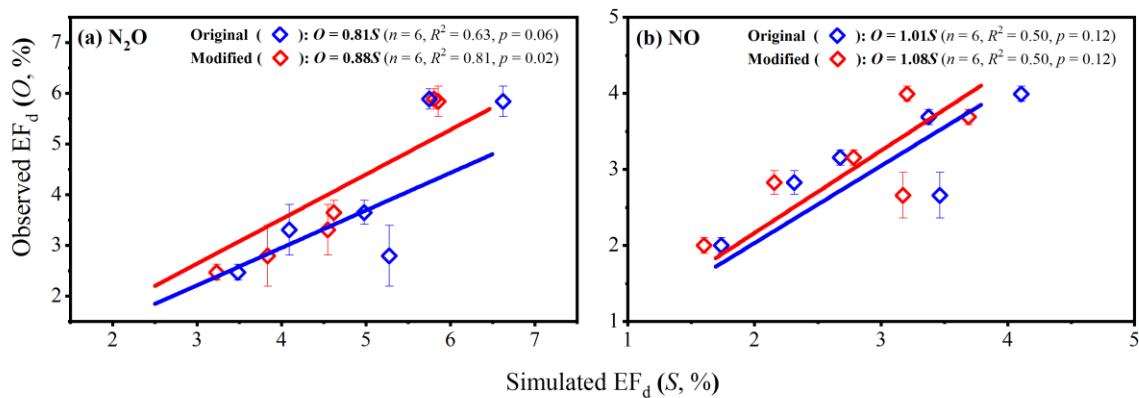
690

691 **Figure 2: Comparison between the observations and simulations of annual nitrous oxide (N₂O) and nitric oxide (NO) emissions.**
 692 **The simulations were provided by the original and modified models. The red or gray solid lines illustrate the zero-intercept**
 693 **univariate linear regressions. The vertical bars indicate the standard error of four spatial replicates. The legends in panel a apply**
 694 **for all panels.**



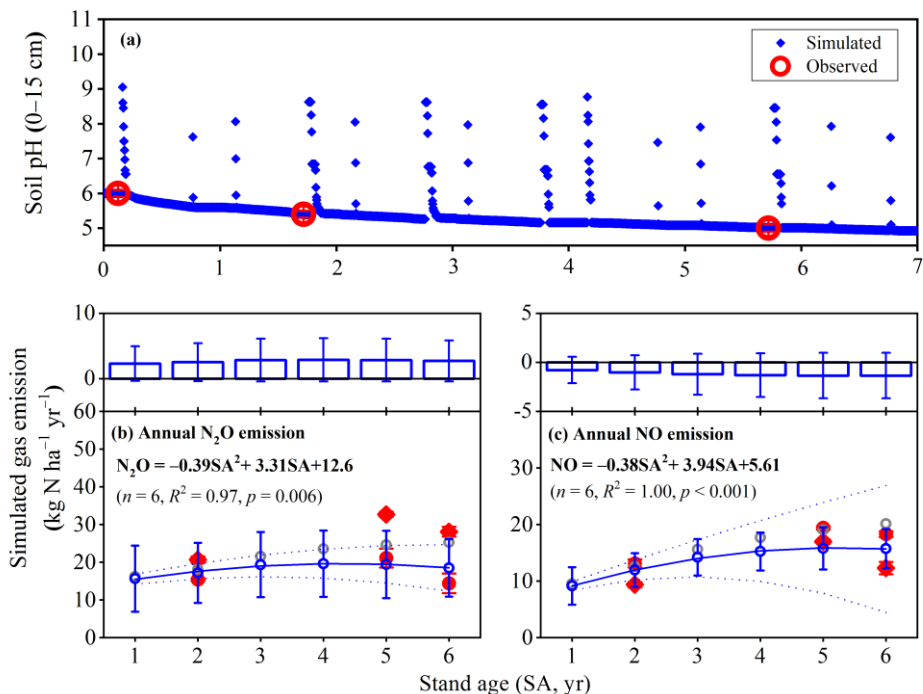
695

696 **Figure 3: Simulated annual emission and direct emission factor (EF_d) of nitrous oxide (N₂O) and nitric oxide (NO) from tea**
 697 **plantations with early stand ages against nitrogen fertilizer doses. Data displayed in panels a–b were simulated by the modified**
 698 **model, and those in panels c–f by the original (grey circle) and modified (blue circle) models. The legends in panel b also apply for**
 699 **panel a, wherein T08 and T12 represent the plantations transplanted with seedlings in 2008 and 2012, respectively, UN and OM**
 700 **indicate the fields consecutively applied with urea since tea planting and short-term replacement of urea with oilcake, respectively,**
 701 **and 2013 and 2014 are the years with field observations of gas emissions. Each vertical bar in panel c–f is the standard deviation of**
 702 **the EF_ds for T08 in 2013 and 2014 and for T12 in 2013. Dashed lines are the lower and upper uncertain bounds at the 95%**
 703 **confidence interval for regression curves. The legends in panel d also apply for panels c, e and f.**



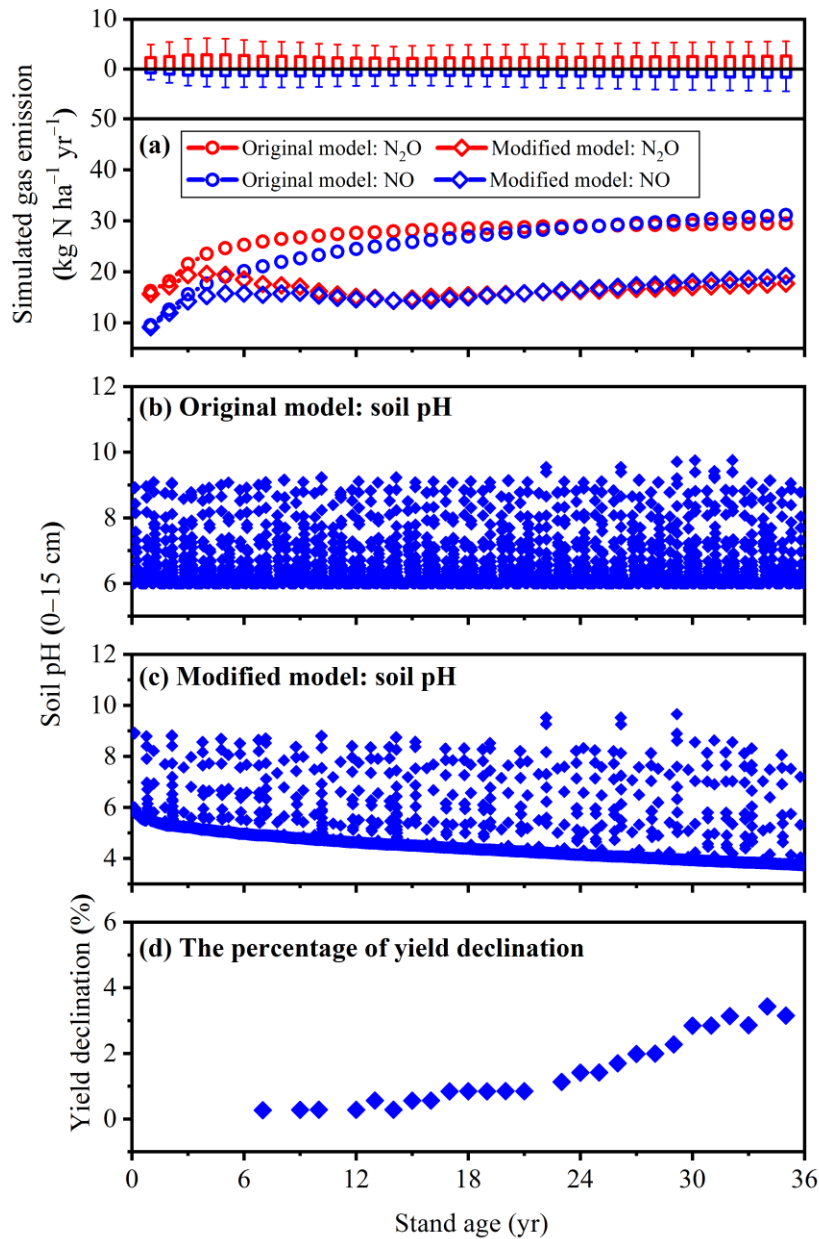
704

705 **Figure 4: Comparison between observed and simulated annual direct emission factor (EF_d) of nitrous oxide (N₂O) and nitric oxide**
 706 **(NO) by the original and modified models from tea plantations. The vertical bar indicates the standard error of four spatial**
 707 **replicates. The blue and red lines illustrate the zero-intercept univariate linear regressions by the original and modified models.**
 708 **Each simulated EF_d is calculated from the simulated emissions of two nitrogen addition levels (zero and 450 kg N ha⁻¹ yr⁻¹).**



709

710 **Figure 5: Simulated topsoil (0–15 cm depth) pH and annual emissions of nitrous oxide (N_2O) and nitric oxide (NO) against early**
 711 **tea stand ages by the modified model. The solid lines were the polynomial regression curves. Dashed lines are the lower and upper**
 712 **uncertain bounds at the 95% confidence interval (CI) for regression curves. Each pH datum is given as the daily mean of eight**
 713 **diurnal simulations (3 h for each). The vertical bar crossing each datum point in panel b or c represents the uncertainty (95% CI)**
 714 **induced by those of model inputs. Each box above panels b–c represents total model error that was estimated by referring to mean**
 715 **of model relative errors (MRBs), with vertical bars representing the uncertainties (95% CI) estimated by referring to the double**
 716 **standard deviations of [MRBs]. The red circle and diamond points in panel b or c represent the observed emissions of N_2O and NO**
 717 **from urea and organic manure treatments. The grey circle point in panel b or c represents the simulation by the original model.**



718

719 **Figure 6: Simulated emissions of nitrous oxide (N₂O) and nitric oxide (NO) and topsoil (0–15 cm) pH of a urea-fertilized tea**
 720 **plantation against stand ages within full lifetime of tea (35 years). Each box above panel a represents total model error of the**
 721 **simulated emissions by the modified model that was estimated by referring to mean of model relative errors (MRBs), with vertical**
 722 **bars representing the uncertainties (95% CI) estimated by referring to the double standard deviations of |MRBs|. The given**
 723 **percentage of yield declination, simulated by the modified model, was due to the effect of soil pH on tea growth.**